ELSEVIER

Agricultural and Forest Meteorology 75 (1995) 1–22

AGRICULTURAL AND FOREST METEOROLOGY

Mean flow and shear stress distributions as influenced by vegetative windbreak structure

R.C. Schwartz[a,*], D.W. Fryrear[b], B.L Harris[a], J.D. Bilbro[b], A.S.R. Juo[a]

[a]*Department of Soil and Crop Sciences, Texas A&M University, College Station, TX 77843, USA*

[b]*Cropping Systems Research Laboratory, Agricultural Research Service, US Department of Agriculture, P.O. Box 909, Big Spring, TX 79720, USA*

Received 12 April 1994; revision accepted 19 September 1994

Abstract

A major deterrent toward arriving at satisfactory estimates of shelter effect of vegetative windbreaks is the difficulty in quantifying permeability to air flow as a function of directly measured physical parameters such as porosity and plant surface area. This weakness seriously limits the accuracy of both empirical and numerical models in describing the effect of vegetative barriers without first knowing some aspects of the induced flow regime. An aerodynamic study of vegetative windbreaks was conducted in a wind tunnel and in the field to assess the effect of barrier structure upon windward and leeward reductions in near ground mean wind speed and surface shear stress. Results from this study show that decreasing windbreak porosities result in reduced or equivalent wind speeds at all leeward distances. An expression was derived to describe the near ground horizontal distribution of mean relative velocity as a function of the leeward minimum relative velocity, the position of this minimum, and surface roughness length. With the exception of the region in the near lee, this model also allows the estimation of the horizontal distribution of shear stress in the vicinity of a barrier. Minimum relative velocities were adequately described as non-linear functions of barrier porosity or projected plant surface area. However, the vertical distribution of porosity with height, largely controlled by plant form, had a major influence on these relationships.

1. Introduction

Wind barriers have long been used to control the erosion of soil by wind. Such barriers reduce soil movement, collect drifting snow, and provide a favorable microclimate for livestock and crops. Although the benefits of wind barriers to agriculture

* Corresponding author.

SSDI 0168-1923(94)02206-2

List of symbols

A_c	effective surface area of leaves and stems per frontal area of barrier ($L^2\,L^{-2}$)
A_l	one-sided surface area of leaves (L^2)
A_s	projected surface area of stems (L^2)
b	barrier width (L)
c_l	coefficient expressing the leeward decay rate of the velocity deficit
c_w	coefficient expressing the rate of increase of the windward velocity deficit
C_{dl}	drag coefficient of a leaf in isolation
C_{ds}	drag coefficient of a stem in isolation
$C_{\tau h}$	shear stress reduction coefficient calculated using u_h
$C_{\tau *}$	shear stress reduction coefficient calculated using u_{*0}
D_s	drag per unit barrier length responsible for reducing shear stress ($M\,T^2$)
d_{s80}	sheltered distance per unit barrier height over which u/u_0 is reduced below 0.8 ($L\,L^{-1}$)
h	barrier height (L)
l	windbreak length (L)
r	row interference parameter which adjusts bulk drag to account for the aerodynamic interference of neighboring rows of plants
Re_t	turbulent Reynolds number $= \ln(h/z_0)/k^2$
u	mean wind velocity ($L\,T^{-1}$)
u_0	mean approach wind velocity ($L\,T^{-1}$)
u_h	mean approach wind velocity at windbreak height ($L\,T^{-1}$)
u_m	minimum mean horizontal wind velocity leeward of a windbreak ($L\,T^{-1}$)
u_*	friction velocity ($L\,T^{-1}$)
u_{*0}	approach friction velocity ($L\,T^{-1}$)
u_{*m}	minimum friction velocity leeward of windbreak ($L\,T^{-1}$)
x	horizontal distance (L)
x_l	parameter corresponding to the intercept of the regression $\ln[(1-u/u_0)/(1-u/u_m)] = c_l x/h - c_l x_l/h$ for $x \geqslant x_m$ (L)
x_m	distance from leeward edge of windbreak to u_m (L)
x_w	parameter corresponding to the intercept of the regression $\ln[(1-u/u_0)/(1-u/u_m)] = c_w x/h - c_w x_w/h$ for $x \leqslant -2h$ (L)
z	vertical distance (L)
z_0	aerodynamic surface roughness length (L)
Greek letters	
α	fitted parameter defined in Eq. (10)
β	fitted parameter defined Eq. (12)
δ	boundary layer depth (L)
ρ	density of air ($M\,L^{-3}$)
τ	shear stress pertaining to the x–z tensor ($M\,L^{-1}\,T^{-2}$)
τ_0	approach shear stress pertaining to the x–z tensor ($M\,L^{-1}\,T^{-2}$)
ϕ	optical porosity of the barrier ($L^2\,L^{-2}$)

are large, no systematic design procedure has been established for vegetative barriers. This is primarily because of the difficulty in interpreting data from field studies and the inability reliably to predict the effect of barrier structure on wind flow modifications and resulting erosion rates. The principal concern of this study was to determine the degree of protection against wind erosion afforded by vegetative windbreaks over a range in plant densities. Within the context of this paper, the interpretation of protection is limited to the distance that friction velocity is reduced below the threshold required to initiate erosion over a given soil surface condition. Therefore, the characterization of the shear stress throughout the upstream and downstream extent of barrier influence is required to adequately evaluate shelter effect upon wind erosion. Several researchers, particularly Hagen et al. (1981) and Wilson (1985), have predicted shelter flow by numerically solving the fluid flow conservation equations using several closure schemes. Both studies, however, consist of predicting flow in the shelter of fences with easily definable characteristics. The analytical theory of Counihan et al. (1974) has limited usefulness, because it does not adequately describe the distribution of shear stress across the wake, the region of most concern for wind erosion effects. Borrelli et al. (1989) used an empirical equation to predict the horizontal velocity distribution leeward of fences with differing porosities. Although this equation is a significant improvement over previous design equations (e.g. Schwab et al., 1981, p. 133), predictions may be inaccurate because the coefficient used to express the effect of porosity was developed using data obtained from essentially two-dimensional objects.

Although many studies have characterized mean flow properties leeward of vegetative barriers, quantitative descriptions of barrier structure needed for aerodynamic interpretations is often lacking. Several researchers (Nageli, 1953; Jensen, 1954; George et al., 1963; Bean et al., 1975) have related the optical porosity of vegetative windbreaks to leeward wind speed reductions. The analysis of Heisler and DeWalle (1988) indicates that optical porosity is closely related to the minimum leeward wind speed and, as such, should be used more often in evaluating the shelter effect of vegetative windbreaks. For vegetative barriers, optical porosity may not always satisfactorily describe the permeability to air flow, because wind flows across three-dimensional spaces and not through two-dimensional openings. Plant characteristics such as leafiness, leaf shape, leaf size, branching habit and stem diameters all have the potential to influence flow leeward of vegetative windbreaks (Bilbro and Fryrear, 1988). The few studies that have measured such plant characteristics in windbreaks (Caborn, 1957; Bean et al., 1975; Maki and Allen, 1978) do not relate them to wind velocity reductions. The importance of plant characteristics has been indirectly demonstrated by Fryrear (1963), who found that the type of windbreak (grain sorghum, sudan grass, forage sorghum and broomcorn, all *Sorghum bicolor* L. Moench) was the major source of the variation in barrier effectiveness. Moreover, much of the variability resulting from plant type was not a result of differences in porosity. In addition to the uncertainty of the influence of plant characteristics on shelter effect, interpretation of results across a range of porosities is limited by differences in the height of wind speed measurements relative to barrier height and differences in the roughness length of the approach wind speed profile (Heisler and DeWalle, 1988). As a result of the above difficulties, the relationship between windbreak structure and shelter has not been satisfactorily documented to ensure optimum design of vegetative barriers.

This paper reports the results of a wind tunnel study and field study of mean flow in the vicinity of prototype forage sorghum (*Sorghum bicolor* L. Moench) and model sorghum and pigeon pea (*Cajanus cajan*) barriers. The specific objectives of this study were (i) to determine the influence of windbreak structure and surface roughness length on the horizontal distribution of friction velocity, (ii) to predict, as simply as possible, the horizontal distribution of near ground velocity and friction velocity windward and leeward of vegetative barriers, and (iii) to compare the results with experimental data in the literature.

2. Materials and methods

2.1. Wind tunnel study

A wind tunnel study was carried out at the USDA-ARS Research Station, Big Spring, TX in a low speed tunnel with a cross-sectional area of 1 m $\times$ 1 m. A turbulence reducing screen was installed at the upstream tunnel entrance to diminish large-scale eddying. Model windbreaks were immersed in a boundary layer 0.3 m deep which was permitted to develop over a smooth surface along an 8 m length of the wind tunnel. The working section consisted of two, 3 m long smooth glass plates placed upstream and downstream of a 60 cm platform used to anchor the model plants. Approach velocity profiles were logarithmic ($P < 0.0001$, $df = 6$) and aerodynamic surface roughness at $x = -1.665$ m averaged 0.016 mm (S.D. = 0.005 mm).

Model forage sorghum and pigeon pea plants (Fig. 1) were used to assemble a total of 24 windbreak designs consisting of varying densities (10.00, 13.33, 16.67 and 20.00 plants per 10 cm of barrier length) and rows (2, 4 and 6). A geometric scale (model to prototype length ratio) of 1:10 was used to design model plants. Sorghum models used in the study were constructed of cloth wrapped wire to serve as stems. Each model sorghum plant possessed nine leaves that were made from ribbon cut from

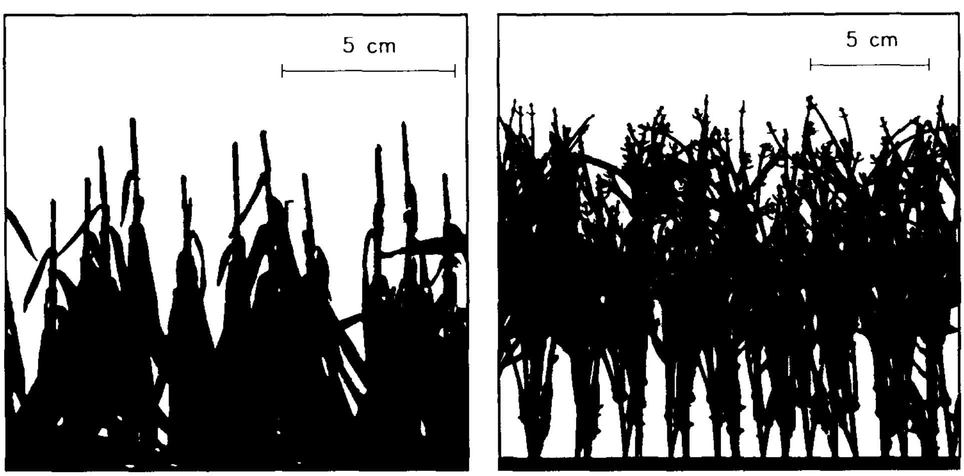

Fig. 1. Silhouette of a model sorghum windbreak (left) and a model pigeon pea windbreak (right) used in the wind tunnel. The sorghum windbreak consists of four rows and has a porosity of 32%. The pigeon pea windbreak consists of two rows and has a porosity of 28%.

patterns. The leaves were glued to the stalk, stiffened with glue and bent downwards to simulate sorghum plants after a killing frost. Sorghum models with leaves not stiffened by glue were evaluated in an additional windbreak design (20 plants per 10 cm of barrier length; two rows). The resulting sorghum models were 10 cm in height, possessed a mean stalk diameter of 0.212 cm and a one-sided leaf surface area of 25.7 cm^2. Pigeon pea models were constructed of plastic coated wire, 15 cm in height and had a mean projected stem surface area of 4.1 cm^2. Model plants were in rows 10 cm apart to simulate prototype 1 m spacings. Intra-row spacings were designed in such a manner so that plants in adjacent rows were not aligned with respect flow normal to the windbreaks. Model windbreaks spanned the entire width of the wind tunnel. A repeated measures design was used such that each experimental unit (windbreak) was subjected to four wind velocities ($u_0 = 5.7,\ 8.0,\ 10.3$ *and* 12.7 m s^{-1} at height $z = 0.1$ m). Optical porosities ϕ ranged from 7 to 39% and were determined using a dot grid to measure the open area to total area ratio from photographs of the middle section of model windbreaks.

Centerline velocities were measured using pitot probes and differential U-tube alcohol manometers in conjunction with temperature and barometric pressure readings. Velocities were recorded at four heights ($z = 0.5,\ 1.0,\ 1.5$ *and* 2.0 cm), at −1.665, −0.6, and −0.3 m from the windward edge and 0.1, 0.2, 0.4, 0.8, 1.2, 1.6, 2.0, 2.4 and 2.8 m from the leeward edge of each model. For multiple row barriers, windward distance was measured from the windward edge and leeward distance was measured from the leeward edge. At the first windward location ($x = -1.665$ m) velocities were also measured at $z = 3.0,\ 4.0,\ 10.0$ *and* 20.0 cm. Relative friction velocities u_*/u_{*0} along the length of the working section were corrected by using the roughness length z_0 obtained from the first windward profile to calculate friction velocity from the profiles at succeeding positions. In the absence of a barrier, this correction set u_*/u_{*0} to near unity (±4%) along the entire length of the working section.

2.2. Field study

Two adjoining, forage sorghum (Pioneer 931) windbreaks 100 m in length were planted in late July, 1990 in an open field at the USDA-ARS Research Station in Big Spring, TX. The windbreaks were oriented north and south and each had four rows spaced 1 m apart. After a freeze severe enough to prevent tillers from forming, sorghum plants were cut to a uniform height of approximately 1 m. Additionally, the soil on both sides of each windbreak was leveled to produce a uniform surface. Lightweight cup (pulse) anemometers (Model 3101, R.M. Young, Traverse City, MI) used in the study were calibrated against a pitot tube and manometer in the wind tunnel and had an average threshold speed of 0.5 m s^{-1} throughout the duration of the study. Anemometers were installed at a height of 0.2 m at 5, 10, 15, 20 and 30 m from the leeward edge of each barrier. A profile of anemometers ($z = 0.2,\ 0.4,\ 0.6$ *and* 1.0 m) was set up 10 m from the windward edge of each barrier. Wind direction was obtained with a wind vane located on the leeward edge of each barrier at a height of 2 m. Mean wind speed and wind direction measurements were sampled continuously by a data logger when prevailing winds were from the west and during periods of adequate wind speed (> 1.5 m s^{-1} at $z = 1$ m) from late November 1990 to mid-April 1991. The two windward rows of the south barrier were removed in December 1990 to allow the evaluation of a two-row windbreak. Data were obtained covering a wide range of wind speeds (10 min means of up to 10.8 m s^{-1} at $z = 1$ m) and a wide range of barrier porosities (0.31–0.72). The average z_0 obtained from approach logarithmic profiles was 2.0 mm (S.D. = 1 mm). Observations of 10 min average wind speeds were included in the analysis provided that the approach logarithmic profile was significant ($P < 0.05$), the mean wind direction did not exceed 15° from perpendicular and the mean approach wind speed at 1 m exceeded 4 m s^{-1}.

Measurements of barrier structure were taken periodically over the duration of the study. As in the wind tunnel study, optical porosity was determined using a dot grid to calculate area on enlarged photos. Top and bottom stem diameters and the height of 30 randomly selected sorghum plants were measured to allow the estimation of stem surface area. The length and width of each leaf on the selected plants were measured to allow a non-destructive estimate of leaf surface area using a previously developed regression equation. The number of plants in the center 30 m of each barrier was recorded. Linear interpolation between measurements over time permitted the estimation of stem and leaf surface area, porosity and barrier density on any given day during the study.

2.3. Computational methods

The total drag per unit barrier length responsible for reducing surface shearing stress D_s was determined using the method of Seginer and Sagi (1972) and is described by

$$D_s = \int_{x_1}^{x_2} (\tau_0 - \tau)\mathrm{d}x \tag{1}$$

where x_1 and x_2, respectively, represent the windward and leeward positions along the x-axis where the logarithmic profiles are equivalent. Here τ_0 and τ are the x-z components of the Reynolds stress tensor for the undisturbed and sheltered flow, respectively. In the wind tunnel, shearing stresses τ_0 and τ and the aerodynamic roughness length z_0 were estimated from the logarithmic velocity profile

$$u = \frac{(\tau/\rho_a)^{\frac{1}{2}}}{k}\ln(z/z_0) \tag{2}$$

where ρ_a is the density of air and k is Von Karman's constant (0.4). In the field, τ_0 was also computed from the logarithmic velocity profile and τ was estimated as

$$\tau = \rho_a u_{*0}^2[u(z)/u_0(z)]^2 \quad z \ll h \tag{3}$$

where h is barrier height, $u_0(z)$ and u_{*0} are velocity and friction velocity, respectively, of undisturbed flow on the windward side of the barrier, u_* is equivalent to $(\tau/\rho_a)^{\frac{1}{2}}$ and $u(z)$ is the velocity along the x-axis. The use of Eqs. (2) and (3) leeward of windbreaks is justified, because the velocity profile that develops over a rough surface in this region should also be logarithmic provided that measurement heights are contained entirely within the wall region (Seginer and Sagi, 1972). In this region only a small portion of the velocity profile deviates from the logarithmic law and there is practically always a constant shear (Plate, 1971; Seginer and Sagi, 1972). The principal difficulty, however, is delineating the leeward position at which the internal boundary layer is well established. Measurements leeward of porous barriers in the wind tunnel (Jensen, 1954) and field (Nageli, 1953) suggest that the logarithmic region is confined to a height of less than $0.5h$ near ($5h$) the barrier. Bradley and Mulhearn (1983) found that drag plate measurements of friction velocity could be estimated by the friction velocity obtained from wind profile measurements at $0.8\ h \leqslant z \leqslant 3.3\ h$ leeward of a 50% porous fence at $25h$ and beyond.

In analogy to a drag coefficient, the shear stress reduction coefficients C_τ for the barrier were computed as

$$C_{\tau h} = D_s / \frac{1}{2}\rho_a u_h^2 h \text{ and } C_{\tau *} = D_s / \frac{1}{2}\rho_a u_{*0}^2 h \tag{4}$$

for each respective characteristic velocity (Seginer and Sagi, 1972). Here u_h is the undisturbed, approach velocity at $z = h$, the height of the barrier. Eq. (1) was numerically integrated from the windward distance where $u_*/u_{*0} = 0.95$ to the leeward distance where u_*/u_{*0} began to exceed 0.95. A cubic spline procedure with the boundary condition of $\mathrm{d}(u_*/u_{*0})/\mathrm{d}(x/h) = 0$ at the most windward position and at $x/h = 60$ was used to interpolate the value of u_*/u_{*0} between the experimental data. This procedure is well suited to interpolations of the horizontal velocity profiles and yields estimates of the minimum relative velocity $u_m(z)$, the location of this minimum along the x-axis x_m, and the sheltered distance over which mean relative velocities are reduced below a specified maximum. In the field the minimum relative velocity u_m was assumed greater than zero (barrier porosities exceeded 30%) and equal to the interpolated minimum wind speed obtained with cup anemometers.

2.4. Conceptual model of shelter effect

The approach we used to estimate shelter effect was to evaluate the rate of recovery of mean relative velocity to the undisturbed, approach velocity in response to differences in barrier structure and surface roughness length. To consider this influence, it is useful to examine the change in mean relative velocity at $z \ll h$ with respect to the leeward distance $x/h - x_m/h$. Assuming that for $x/h > x_m/h$ the rate of return of mean velocity to equilibrium is proportional to the velocity deficit, the boundary condition $u(z)/u_0(z) \to 1$ as $x/h \to \infty$ leads to

$$\frac{\mathrm{d}[u(z)/u_0(z)]}{\mathrm{d}[x/h - x_m/h]} = c_1\left(1 - \frac{u(z)}{u_0(z)}\right) \tag{5}$$

where c_1 is a rate constant defining the leeward decay of velocity reductions.

Separating the variables, integrating with the additional boundary condition that $u(z)/u_0(z) = u_m(z)/u_0(z)$ at $x/h = x_m/h$, and solving for $u(z)/u_0(z)$ yields

$$\frac{u(z)}{u_0(z)} = 1 - \left(1 - \frac{u_m(z)}{u_0(z)}\right) \exp[-c_1(x/h - x_m/h)] \quad x/h \geqslant x_m/h$$
$$\frac{u(z)}{u_0(z)} < 1 \quad z \ll h \tag{6}$$

While Eq. (6) is similar to the empirical equation of Borrelli et al. (1989), the displacement of x/h by x_m/h ensures that c_1 is evaluated at leeward positions where $\mathrm{d}(u(z)/u_0(z))/\mathrm{d}(x/h)$ is always positive. Evaluation of c_1 leeward of $x/h = 0$ will force the constant of integration to be dependent upon x_m. In addition, without adequate substantiation, the coefficient c_1 can only be considered to be constant for a given barrier under specific surface and wind conditions. Although Eq. (6) makes over-simplified assumptions about the horizontal distribution of velocity in the lee of a wind barrier, it does allow the experimental determination of the decay constant and the evaluation of its dependency upon barrier structure and surface roughness length.

3. Results and discussion

3.1. Air flow modifications

Large scale eddying behind dense ($\phi \leqslant 21\%$) model sorghum barriers was evident by reverse flows detected by pitot probes at leeward distances of $4h$ and $8h$ (Fig. 2). These results agree well with the findings of Perera (1981), who demonstrated the presence of recirculating flows leeward of fences with porosities of 30% and less using the more sensitive pulse-wire anemometer. Recirculation zones were not detected leeward of model pigeon pea barriers. Apparently, the jetting of air through the gaps in the lower portion of these barriers (Fig. 2) discouraged the formation of large scale eddies.

The velocity profiles measured at windward and leeward positions along the x-axis in the wind tunnel permitted the evaluation of the degree to which they conformed to the logarithmic equation. Velocity profiles windward of both model sorghum and pigeon pea barriers were logarithmic ($P < 0.05$) at all distances measured over the range in porosities examined (7–39%). Normalized velocity profiles at positions along the x-axis for selected windbreaks are shown in Fig. 2. Assessment of all wind tunnel results indicates that the leeward distance required for the establishment of a logarithmic ($P < 0.05$) velocity profile decreases as porosity increases. The velocity profile at $z \leqslant 0.20h$ was in most cases logarithmic at close distances ($4h$) leeward of model sorghum barriers with porosities exceeding 30%. All profiles were logarithmic at $x \geqslant 4h$ leeward of the most porous sorghum windbreak (37%). Velocity profiles at $z \leqslant 0.13h$ leeward of model pigeon pea barriers were well described by the logarithmic relationship at even closer distances, in part, due to a lower relative height of measurement. Moreover, higher velocities near the surface and lack of a

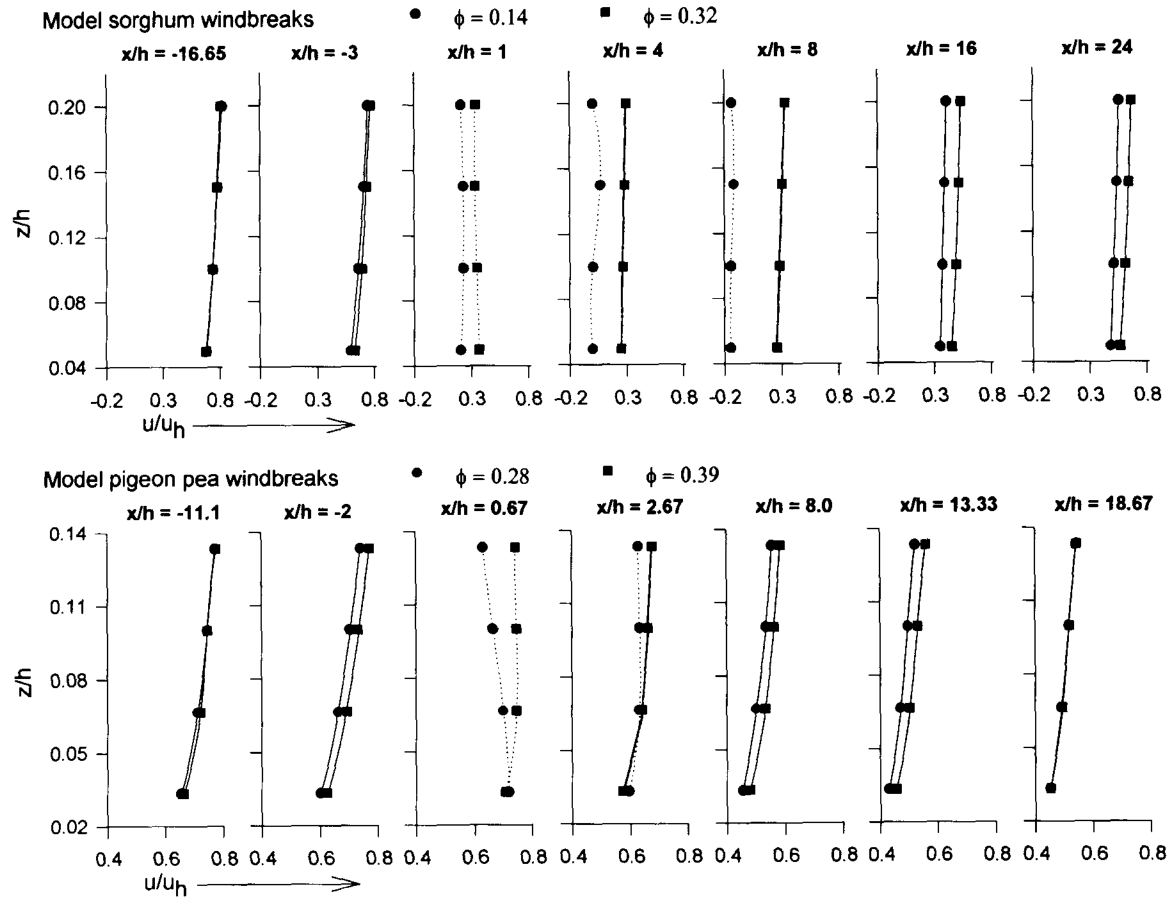

Fig. 2. Normalized velocity profiles obtained in the wind tunnel along the x-axis for selected windbreaks. Solid lines indicate profiles are significantly ($P < 0.05$) logarithmic. The corresponding sorghum and pigeon pea barriers with porosities of 32% and 28%, respectively, are shown in Fig. 1.

recirculation zone leeward of model pigeon pea barriers promoted a more rapid re-establishment of the logarithmic profile (Fig. 2).

Evaluations of velocity profiles confined to $z \leqslant 0.4h$ leeward of porous windbreaks ($\phi > 30\%$) are uncommon; however, wind tunnel measurements leeward of 48% porous fence by Jensen (1954) support the results of this study and demonstrate the re-establishment of a logarithmic profile by $x \approx 4h$. Fig. 2 also shows that a distance of up to $16h$ is required for the re-establishment of logarithmic velocity profiles leeward of dense ($\phi \leqslant 0.2$) windbreaks. This distance compares favorably with the flow reattachment points measured by Raine and Stevenson (1977) ($9h$) and Ogawa and Diosey (1980b) (6–$12h$) for solid and dense fences. For the aerodynamically rougher surfaces in the field (i.e. $h/z_0 < 2000$), the leeward distance required for the establishment of a well defined logarithmic velocity profile would be expected to be smaller than the distances obtained by this study in the wind tunnel. A larger z_0, in effect, would promote the generation of larger eddies (and hence a larger turbulent transport coefficient) and facilitate a more rapid re-establishment of open wind velocities. This concept is supported by experimental evidence of Ogawa and Diosey (1980a,b) that demonstrates the leeward distance to the point of reattachment increased as h/z_0 increased.

Given the above evidence for porous ($\phi > 30\%$) barriers, velocity profiles windward of $-2h$ and leeward of $4h$ are approximately logarithmic below $0.2h$. Hence, with accurate velocity profile measurements in these regions, u_* can be evaluated.

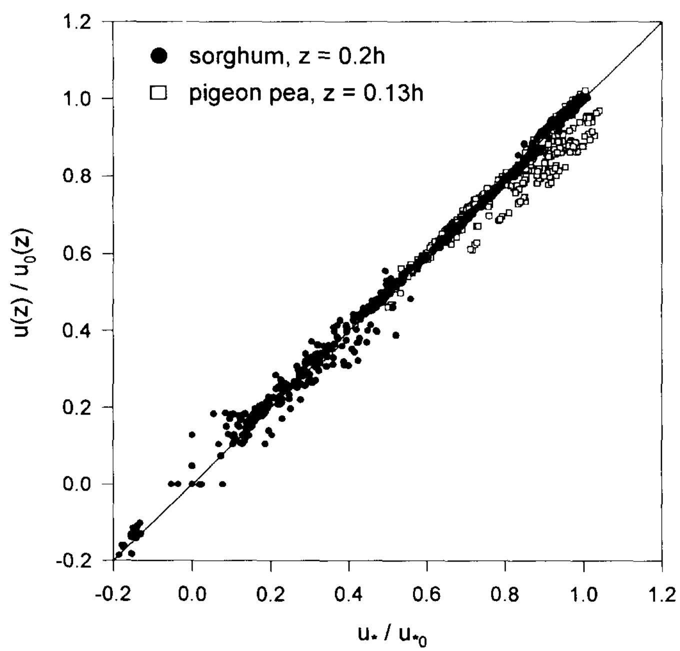

Fig. 3. Comparison of near-wall mean relative velocities with friction velocities at windward and leeward distances from model sorghum and pigeon pea barriers in the wind tunnel. Line shown is 1:1.

Assuming that z_0 remains relatively constant throughout the region of barrier influence, u_* also can be estimated from a single velocity measurement at or below $0.2h$ and the undisturbed approach friction velocity u_{*0}. The magnitude of error introduced into the estimation of u_*/u_{*0} by using $u(z)/u_0(z)$ measured at $z = 0.2h$ rather than the entire profile below $0.2h$ is small and approximates a 1:1 relationship (Fig. 3). The systematic deviation of u/u_0 from u_*/u_{*0} at high relative velocities (Fig. 3) is a result of the small or often negative velocity gradients generated in close proximity to pigeon pea barriers (Fig. 2). Velocity profiles leeward of pigeon pea windbreaks also may have been influenced by a boundary layer depth (δ) of only $2h$. Although a ratio of h/δ less than 0.3 is generally required to maintain flow independence from boundary layer depth, Good and Joubert (1968) found that for h/δ less than 0.5, the effects of outer flow variables upon solid plate drag coefficients were small, presumably because the downward rate of momentum transport is relatively slow. The sensitivity of $C_{\tau *}$ or velocity profiles to outer flow variables in this study would therefore be expected to be minor because measurements were taken very close to the wall. Estimates of τ obtained from Eq. (3) permit the computation of surface shear stress reduction coefficients $C_{\tau h}$ and $C_{\tau *}$ provided that an adequate number of velocity measurements are taken at $z \leqslant 0.2h$ along the x-axis. Because of the uncertainty of friction velocity values obtained from an assumed logarithmic distribution in the region $-2h \leqslant x \leqslant 4$–$8h$, calculated values of $C_{\tau h}$ and $C_{\tau *}$ are only approximations.

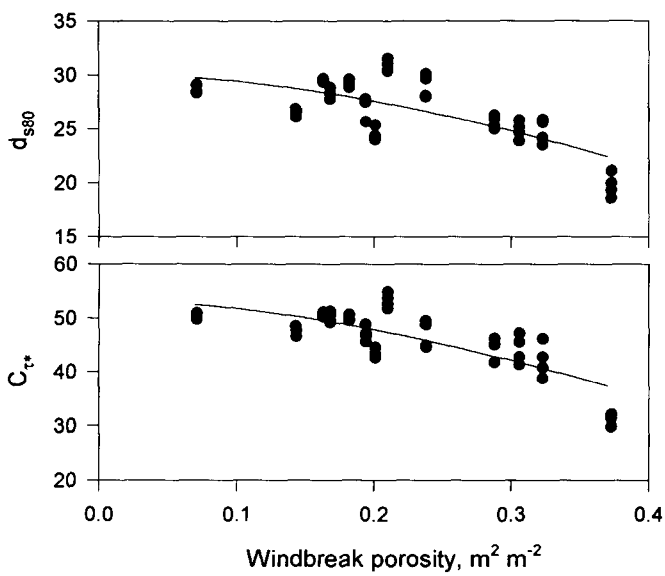

Fig. 4. Influence of model sorghum windbreak porosity on sheltered distance (d_{s80}) and the shear stress reduction coefficient ($C_{\tau *}$) in the wind tunnel.

3.2. Shelter effect

The magnitude of $C_{\tau h}$ and $C_{\tau *}$ obtained for model sorghum barriers in the wind tunnel and forage sorghum in the field compares favorably with those of Seginer and Sagi (1972), Miller et al. (1975) and Seginer (1975). Both wind tunnel and field results of this study indicate that $C_{\tau h}$ is more sensitive than $C_{\tau *}$ to variations in the approach mean wind speed and the turbulent Reynolds number Re_t at $z = h$.

In agreement with the analyses of Wilson (1985) and Heisler and DeWalle (1988), wind tunnel and field results show an increasing downstream extent of wind reductions as barrier porosity is decreased. The wind tunnel results (Fig. 4), however, demonstrate that decreasing windbreak porosities beyond 20% do not generate significant increases or decreases in sheltered distance (d_{s80}). The variation of sheltered distance and $C_{\tau *}$ with barrier density for the model sorghum windbreaks shown in Fig. 4 suggest that maximum shelter effect is obtained with porosities of approximately 20%. Raine and Stevenson (1977) also found that the best overall wind velocity reduction in their study was given by a 20% permeable fence. Although measures of sheltered distance and $C_{\tau *}$ could not be reliably estimated for pigeon pea barriers (because leeward velocity measurements were restricted to $x/h \leqslant 18.67$), mean relative velocities resulting from these barriers were greater than those of model sorghum windbreaks of similar porosities throughout the entire leeward distance measured.

3.3. Decay of the velocity deficit

The rate of recovery of leeward friction velocity to the undisturbed, approach friction velocity in the wind tunnel is well described by Eq. (6) ($R^2 > 0.96$, $n \geqslant 6$). However, the leeward displacement from the barrier is not described by x_m/h but rather by x_l/h, which roughly corresponds to the maximum extent of the quiet zone leeward of dense barriers (Fig. 5). Wind tunnel results indicated that x_l can be reliably estimated ($R^2 = 0.95$, $n = 62$) as a function of x_m and yields

$$x_l/h = 1.5 + 0.92 x_m/h \tag{7}$$

Although the equation proposed by Borrelli et al. (1989) fits equally well, the constant of integration in their analysis (A), was often more than double that denoted to be the maximum corresponding to the barrier drag of solid barriers. Hence, the variable A cannot be solely dependent upon barrier porosity or barrier drag.

Multivariate analysis of variance indicates that the leeward decay rate of the velocity deficit c_l is not significantly ($P < 0.05$) influenced by barrier width, intra-row spacing and approach velocity. The lack of response of the decay coefficient to changes in barrier density is also suggested by the numerical results of Wilson (1985). Wilson's second order closure scheme (1985; Fig. 9) shows that relative velocities generated leeward of barriers with different pressure loss coefficients tend to converge at distances far downstream. Results presented by Raine and Stevenson (1977) also show no systematic deviation of the decay coefficient with porosity. Examination of Fig. 5 seems to suggest that the insensitivity to porosity and hence

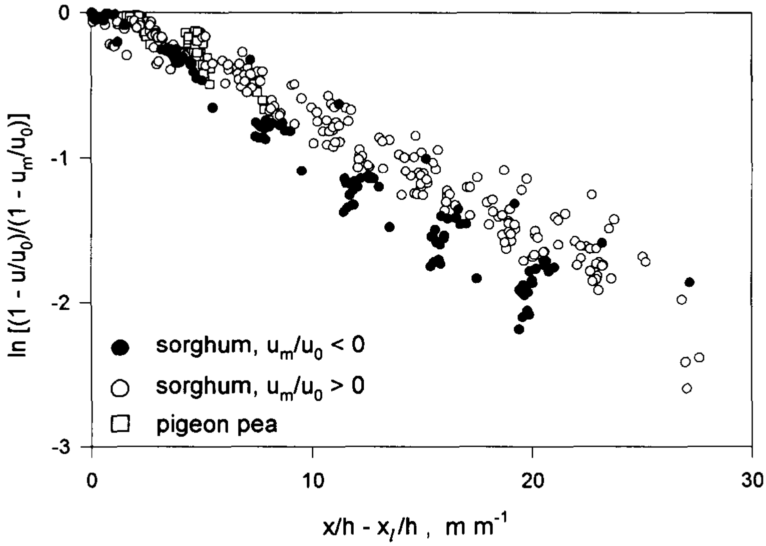

Fig. 5. Mean relative velocity measurements leeward of model sorghum and pigeon pea barriers in the wind tunnel plotted in terms of scaled variables.

$u_m(z)$ is valid only for $u_m(z)/u_0(z)$ greater than 0. However, this is principally a result of large values of x_m at low porosities which force regression estimates of $|c_l|$ to be larger. The net result is that barriers generating minimum relative velocities less than zero yield similar velocity reductions in the far lee as barriers with $u_m(z)/u_0(z) \approx 0$. This may explain a portion of the leveling out of sheltered distance and C_{T*} at porosities less than 0.2–0.3 in Fig. 4.

The rate of recovery of the leeward velocity to the undisturbed, approach velocity in the field is also well described by Eq. (6), although with a larger degree of variability in c_l than exhibited by the wind tunnel results. Some variability was caused by the interaction of the incidence angle with large gaps in porous (> 0.7) barriers and variations in the roughness length manifested in the approach wind speed profiles. Although changes in atmospheric stability may be responsible for some of the variability at low wind speeds, daily fluctuations which would suggest such a dependence are not evident. Most of the variability was likely caused by the linearization of Eq. (6), which produces weighting in favor of far downwind locations. An imperfect spatial correlation or small (±2%) error in wind speed measurement at locations far downwind would therefore yield larger errors in c_l estimated from the regression equation. Analogous to the wind tunnel results, however, c_l was not sensitive to changes in barrier porosity.

Several investigations and reviews (Jensen, 1954; Van Eimern et al., 1964; Counihan et al., 1974; Wilson, 1985; Heisler and DeWalle, 1988) have demonstrated that the reduction in the ratio h/z_0 results in a decrease in the extent of mean velocity reductions leeward of a barrier. In the constant flux layer under near-neutral conditions, $\ln(h/z_0)$ is proportional to the turbulent Reynolds number and sets the scale of turbulence under averaged motion. It is therefore reasonable to assume that c_l should be a function of $\ln(h/z_0)$ because it governs the rate of return of u/u_0 to open wind speed. A comparison of results obtained from this study with those of Nageli (1953), Woodruff et al. (1963), Seginer (1975) and Raine and Stevenson (1977) is shown in Fig. 6. These studies were selected because all report fractional velocity reductions at $z \leqslant 0.5h$ provide reasonable estimates of z_0 as obtained from the undisturbed velocity profile. For these sets of experiments, which cover a wide range in h/z_0 and porosity, c_l varies linearly with $\ln(h/z_0)$ and is described by

$$c_l = \ln(h/z_0)/120 - 0.16 \tag{8}$$

with a significant ($P < 0.001$) slope and intercept. This suggests that the variation in c_l is primarily governed by $\ln(h/z_0)$. These results confirm that increased surface roughness as scaled by barrier height will reduce the shelter effect of a given windbreak by increasing the rate of return of velocity to open wind speed.

Windward velocity reductions in the wind tunnel were also examined and fitted to Eq. (6). With a few exceptions, the slopes were significantly different from zero ($P < 0.05$); however, the overall fit was poorer than that obtained for the leeward case. The horizontal displacement corresponding to the fitted intercept was approximately located at the leeward edge of barriers and could be roughly described

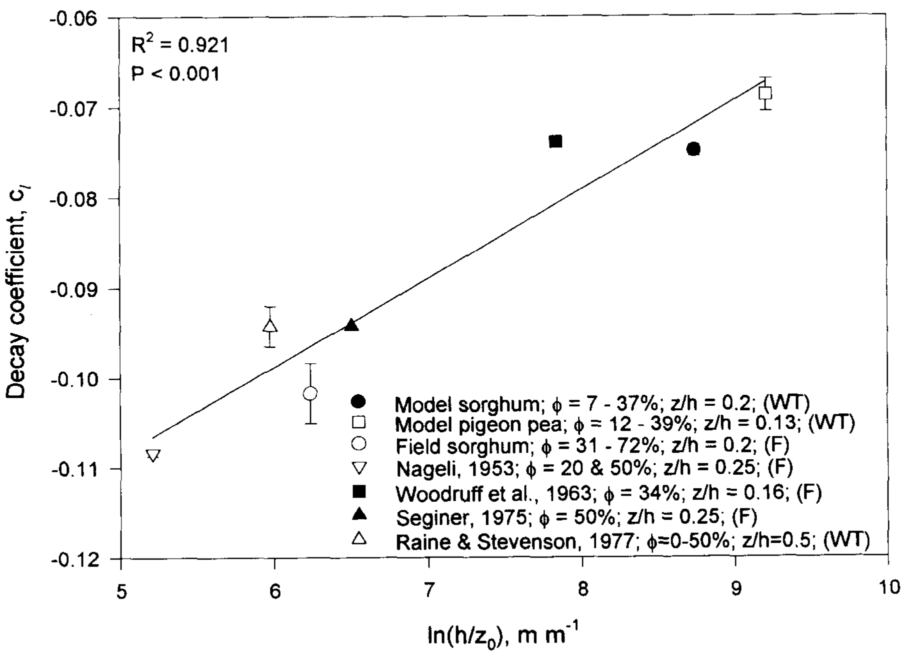

Fig. 6. Dependence of the decay coefficient c_l upon h/z_0 for this research and other studies in the field (F) and wind tunnel (WT). Surface roughness z_0 for Raine and Stevenson (1977) and Woodruff et al. (1963) was obtained from velocity profiles in their Figs. 2 and 4, respectively. Error bars indicate standard error of the mean.

as

$$x_w = 0.11 x_m \tag{9}$$

($R^2 = 0.81$), omitting outliers from non-significant regressions. The rate of increase of windward velocity deficits c_w averaged 0.7 for pigeon pea and 0.5 for sorghum barriers, while windward measurements obtained by Nageli (1953) give a mean value of $c_w = 0.4$. These three data sets suggest that the rate of increase of windward velocity deficits increases with decreasing h/z_0. Although this interpretation seems reasonable, there are insufficient data in the literature to substantiate it. Nonetheless, the horizontal shear stress distribution is not particularly sensitive to changes in c_w which produce a maximum deviation of predicted $C_{\tau *}$ by ±5% for barriers with $\phi \leqslant 0.7$.

3.4. Prediction of the horizontal velocity distribution

Windward and leeward reductions in wind speed were computed using Eq. (6) with measured values of $u_m(z)$, x_m and h/z_0 obtained from studies in the literature (all with $z \leqslant 0.5h$). For $x \leqslant -2h$, the exponent in Eq. (6) was replaced with $c_w(x/h - x_w/h)$, using $c_w = 0.6$ obtained from the mean of wind tunnel results and x_w evaluated using Eq. (9). For $x \geqslant 1.5x_l$, the exponent was replaced with $c_l(x/h - x_l/h)$ using x_l and c_l as computed from Eqs. (7) and (8), respectively. A cubic spline procedure was used with the known value of $u(z)/u_0(z)$ at x_m and the derivative of Eq. (6) at the endpoints to obtain estimates of $u(z)/u_0(z)$ in the region $-2\text{h} < x < 1.5x_l$. Predicted values of $u(z)/u_0(z)$ compare satisfactorily with measured values ($R^2 = 0.97$) and yield a slope of 1.01 (Fig. 7). Inspection of selected data sets indicates that the rate of recovery of $u(z)/u_0(z)$ to unity in the far lee is accurately predicted. This includes independent experimental data (e.g. Perera, 1981) as well as data utilized to predict c_l as a function of h/z_0 in Fig. 6. Leeward velocity reductions were consistently underestimated within the region $10h < x < 20h$ for some data sets, most notably those of Raine and Stevenson (1977). However, this may result from instrumental error of measuring $u_m(z)/u_0(z)$ using hot-wire anemometers which have been shown consistently to overestimate relative velocities in the near lee and as far downstream as $22h$ (Perera, 1981). Given estimates of $u_m(z)$ and x_m and with a knowledge of local surface roughness conditions, Eq. (6) as formulated above yields the horizontal distribution of mean relative wind speeds at $z \leqslant 0.5h$. Additionally, estimates of friction velocity can also be obtained using Eq. 3 for porous ($\phi \leqslant 0.3$) windbreaks in the regions where $x < -2h$ and $x > 4h$.

The principal requirement of the above approach to estimate the horizontal velocity distribution is the proper evaluation of $u_m(z)$ and x_m. Using a numerical model to simulate shelter flow, Wilson (1985) found that the fractional reduction in wind speed at the location of the minimum was insensitive to changes in h/z_0. Although multivariate analysis of variance for the wind tunnel data demonstrates that $u_m(z)/u_0(z)$ increases with increasing approach velocity, the slope of the curve is slight and generates an average increase in $u_m(z)/u_0(z)$ of less than 0.03 over the range

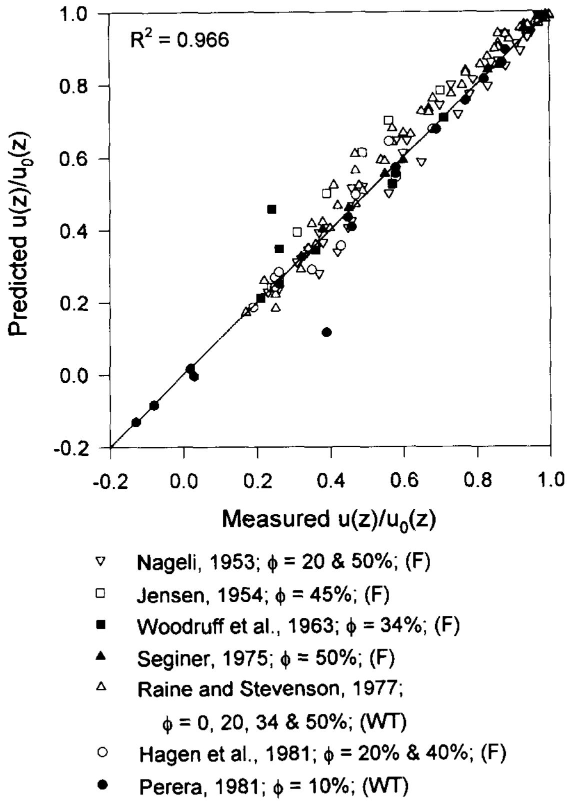

Fig. 7. Comparison of measured and predicted $u(z)/u_0(z)$ for several studies in the field (F) and wind tunnel (WT). Line shown is 1:1.

of velocities examined (5.7–12.7 m s^{-1} at $z = 0.1$ m). Atmospheric instabilities can also influence $u_m(z)/u_0(z)$, as indicated by Seginer (1975); however, these effects would be minor under conditions when protection close to the surface is important (e.g. sufficiently high velocity gradients near the surface to render a Richardson number close (± 0.2) to zero). Daily variations in the magnitude of $u_m(z)/u_0(z)$ leeward of sorghum windbreaks in this study are principally a result of deviations in wind direction because of a non-uniform plant density along the length of the barrier. Large variations (10%) in $u_m(z)/u_0(z)$ reported by Seginer (1975) are not evident in our field data when the effects of wind direction are taken into account. Under the conditions of our study ($z \leqslant 1$ m, $\partial u/\partial z > 0.64 s^{-1}$), however, atmospheric stability effects would be expected to be small.

Under conditions when protection against wind erosion is important, variations of $u_m(z)/u_0(z)$ velocity resulting from atmospheric instabilities and approach wind speed would be relatively small when compared with the effect of barrier permeability. For barriers with a uniform porosity and a width $b \ll h$, the evaluation of $u_m(z)$ is straightforward and can be estimated as a function of a resistance coefficient using the aid of equations such as those of Wilson (1985). The minimum velocity may also be evaluated as a function of optical porosity for fences; however, the relationship shown by Heisler and Dewalle (1988; Fig. 6) is probably in error because of overestimation of velocities by hot-wire anemometers and the inability of cup anemometers to detect reverse flows. Utilizing data in the literature obtained with cup anemometers for $\phi > 0.3$ (Nageli, 1953; Jensen, 1954; Seginer, 1975; Hagen et al., 1981) and pulsed-wire anemometers (Perera, 1981) and pitot-static tubes (Baltaxe, 1967) for barriers of negligible width, the minimum relative velocity can be described as

$$\frac{u_m(z)}{u_0(z)} = 1 - 1.25(1-\phi)^{\alpha} \tag{10}$$

with $\alpha = 0.86$ and an R^2 of 0.97 (Fig. 8). For 'three-dimensional' natural windbreaks, however, the relationship between optical porosity and $u_m(z)/u_0(z)$ is obviously less clear (Fig. 8). Extrapolation of the apparent linear relationships for $u_m(z)/u_0(z) \leqslant 0.6$ in Fig. 8 yields a minimum relative velocity of -0.18 for model pigeon pea and -0.22 for model and prototype sorghum barriers, both of which are quite close to the value of -0.25 for solid fences as measured by Perera (1981). Hence, Eq. (10) also describes the variation in minimum velocity for field and wind tunnel sorghum barriers with a fitted coefficient of $\alpha = 1.51$. This agrees quite closely with $\alpha = 1.45$ obtained from

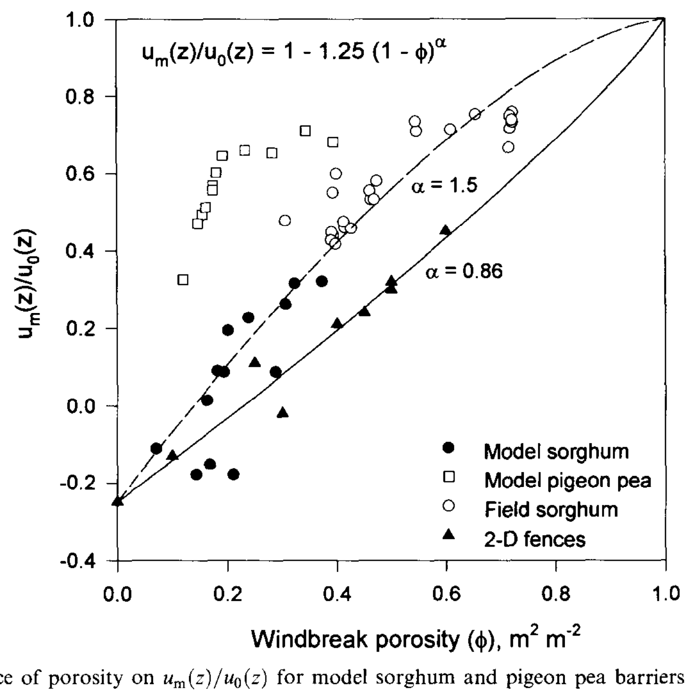

Fig. 8. Influence of porosity on $u_m(z)/u_0(z)$ for model sorghum and pigeon pea barriers (means across velocities), field sorghum barriers (daily means) and two-dimensional fences. Data for two-dimensional fences are those of Nageli (1953), Jensen (1954; Fig. 180), Baltaxe (1967; Table 1), Seginer (1975; Fig. 9(a)), Hagen et al. (1981; Fig. 3), and Perera (1981; Fig. 3).

the data of George et al. (1963), Sturrock (1969) and Bean et al. (1975) for barriers exceeding 30% porosity and not relatively open near the surface. This is despite the fact that these barriers ranged in width from less than $1h$ to $2.2h$ and consisted of tree species with forms differing greatly from each other and sorghum plants. The relationship exhibited for pigeon pea models is substantially different from sorghum models and plants. This may be a result of the difference in the porosity profile although use of the lower half or lower third of the barrier porosity as an index of $u_m(z)$ did not substantially improve the relationship between the two plant types.

For practical applications, it is often necessary to obtain information regarding barrier structure before planting and throughout the growing season. Models simulating plant growth, however, are adapted to predict stem diameters and leaf surface area rather than optical porosities. The influence of plant surface area upon the minimum relative velocity may be attributed to an effective surface area A_e that can be parameterized as

$$A_e = \left(\frac{C_{ds} A_s + C_{dl} A_l}{h \cdot l} \right) \cdot r^{b/h} \tag{11}$$

where n is the number of windbreak rows; A_s and A_l are the projected area of stems (diameter × length) and leaves (one-sided surface area) over a given length l of barrier and C_{ds} and C_{dl} are the weighted drag coefficients of the respective component in isolation. In addition, r^{n-1} is a factor that adjusts the bulk drag coefficient to account for the aerodynamic interference of neighboring rows of plants. Although the drag coefficient is dependent upon wind speed (and therefore upon z and elasticity of components) (Thom, 1971), this leads to excessive complexity and, because of the general lack of measurements that characterize these responses, A_e was evaluated assuming Reynolds number and height independence. The dependence of $u_m(z)/u_0(z)$ on A_e can be expressed by an exponential relationship of the form

$$\frac{u_m}{u_0} = 1.25 \exp(-\beta A_e) - 0.25 \tag{12}$$

where β is a fitted coefficient. An average row interference factor of 0.87 was used to evaluate A_e because r varied little (±5%) between model sorghum, model pigeon pea and prototype sorghum barriers. Assuming that a C_{ds} of 1.0 is a reasonable estimate for rigid cylindrical stems (Thom, 1971; Hagen, 1988), normalization of model sorghum and pigeon pea data with β = constant requires that $C_{dl} = 0.26$. A plot of the field and normalized wind tunnel data with β constant are shown in Fig. 9. The derived drag coefficient for the stiff leaved sorghum plants approaches the maximum of 0.30 obtained by Den Hartog (1973) for isolated corn leaves at normal incidence. Considering that (1) the lateral interference factors would be greater for leaves than stems and (2) deviation of the angle of incidence from right angles would reduce the drag coefficient of leaves to a greater degree than stems, the derived drag coefficient for leaves is probably overestimated. This would suggest that the coefficient β is not constant and here it is suspected that β varies with the vertical distribution of porosity. There are no known data of projected plant surface areas with which to compare our results for $u_m(z)/u_0(z)$; however, numerical and experimental evidence

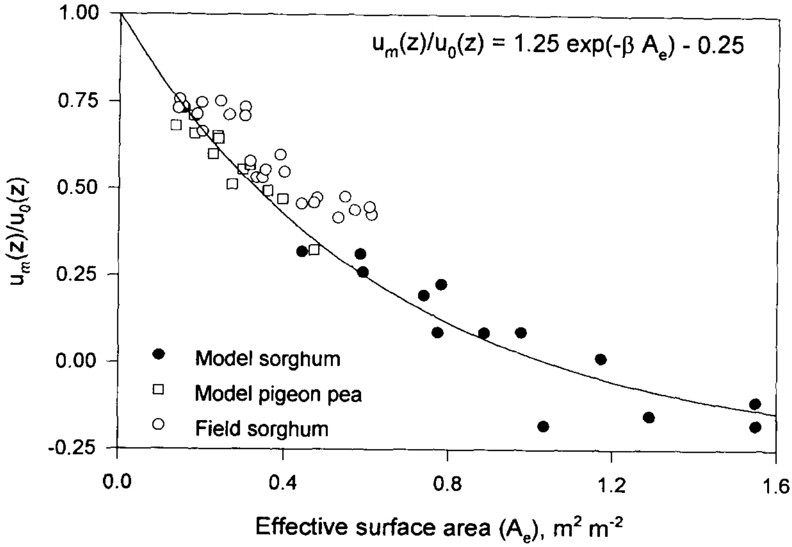

Fig. 9. Influence of effective plant surface area A_e on $u_m(z)/u_0(z)$ for model sorghum and pigeon pea barriers (means across velocities) and field sorghum barriers (daily means). Curve shown is best fit for model sorghum and pigeon pea barriers with the assumption of $C_{ds} = 1$.

from Wilson (1987) lend support to this interpretation. The poor fit between the model and field plants (Fig. 9) also indicates that β will vary with growth form; however, measured values of $u_m(z)/u_0(z)$ in the field are probably overestimated because of the sparse placement of anemometers in the near lee.

Results obtained in the wind tunnel indicate that x_m/h was primarily dependent on plant type. Values of x_m/h from model pigeon pea barriers were, on the average, two to three times larger than those of model sorghum barriers. For sorghum barriers, x_m/h decreased with increasing porosity while for pigeon pea barriers the reverse effect was observed. Some of these inconsistencies may have resulted from an improper scaling of plant models with regard to boundary layer depth. Castro and Fackrell (1978) demonstrated that the magnitude of the reattachment point leeward of solid flat plates is independent of boundary layer depth when h/δ is less than 0.3–0.4. Above this range, the reattachment point moves downstream with increasing h/δ. The implications of these findings on the present study is not clear, because reattachment points do not exist for many porous barriers and the pressure distribution on the barrier face is substantially modified because of variations in porosity with height. Changes in x_m/h as a function of porosity are similarly inconsistent in the literature (Sturrock, 1969, 1972; Bean, et al., 1975; Heisler and DeWalle, 1988). At low z/h and under field conditions, however, the porosity dependence is not evident and x_m/h rarely exceeds 6 m m^{-1} (Nageli, 1953; Woodruff et al., 1963; Sturrock, 1969; Hagen and Skidmore, 1971; Sturrock, 1972; Bean et al., 1975; Heisler and DeWalle, 1988). Furthermore, published photos of Sturrock (1969, 1972) suggest that x_m/h is principally a function of the barrier porosity near the surface relative to the porosity of the entire barrier. From these photos, x_m/h ranges from 2 to 4, 4 to 5, and 5 to 7 for barriers categorized as relatively dense, uniform and open near the base, respectively. Within each of these ranges, the maximum error associated with the prediction of $C_{\tau*}$ is only ±3% for barriers with $\phi \leqslant 0.7$.

4. Conclusions

An aerodynamic study of wind barriers was conducted in a wind tunnel and under field conditions to assess the effect of barrier structure upon windward and leeward reductions in mean velocity and surface shear stress. Approach wind flow characteristics were described in the field and in the wind tunnel using the logarithmic profile as determined from velocity measurements at several heights. Velocity measurements were also taken at several locations windward and leeward of barriers to allow the evaluation of barrier effect. The experimental measurements of airflow about barriers used in this investigation and the subsequent analyses of selected data in the literature with the model developed from this work support the following conclusions.

The logarithmic profile below a height of $0.2h$ in the wind tunnel was valid at all windward distances measured and also at leeward distances greater than or equal to $4h$ for model sorghum barriers with porosities greater than 30%. Most velocity profiles were logarithmic at $12h$ and at greater distances leeward of denser sorghum barriers. For the aerodynamically rougher surfaces in the field, the leeward distance required for the establishment of a well defined logarithmic velocity profile within the new boundary layer would be expected to be smaller at all barrier porosities. Consequently, it is reasonable to expect that surface shear stresses computed from the velocity profiles in the field below a height of $0.2h$ beyond these leeward distances are acceptable estimates under these conditions. Hence, mean relative velocities measured below $0.2h$ are approximately equal to relative friction velocities in these regions if the roughness length can assumed to be constant.

Measurements from this study indicate that decreasing windbreak porosities result in reduced or equivalent wind speeds at all x/h. Decreasing barrier porosities below 20%, however, did not result in significant increases or decreases in sheltering benefits as measured by sheltered distance and the shear stress reduction coefficient ($C_{\tau*}$). This range in porosities (0–20%) corresponds to reverse flow immediately leeward of model sorghum barriers. The presence of a relatively porous region near the base of pigeon pea barriers reduced the sheltering effect of these windbreaks substantially.

By assuming that the rate of return of leeward velocity to equilibrium is proportional to the velocity deficit, Eq. (6) was developed to describe the near ground horizontal distribution of mean relative velocity in the vicinity of a barrier. This equation fits the wind tunnel and field results from this study well. In addition, comparison of model results with published data ($z \leqslant 0.5h$) suggests that this equation has relatively good predictive capabilities. The natural logarithm of the ratio of windbreak height to surface roughness length, $\ln(h/z_0)$, was found to be a valid scaling variable between leeward shelter effects over surfaces of differing roughness and allowed the description of self-similar flows using the developed model. These results confirm that a smaller h/z_0 will reduce the shelter effect of a given windbreak by increasing the rate of return of velocity to approach conditions. With the exception of the region in near lee, this model allows the estimation of the horizontal distribution of shear stress which is the first step in the prediction of wind erosion rates in the vicinity of windbreaks.

A practical weakness of the model used in this study is the difficulty in expressing the minimum relative velocity as a function of barrier structure. For fences with a relatively uniform porosity, estimates of the maximum velocity reduction are well described as a function of porosity. Porous vegetative barriers, however, yield larger minimum relative velocities than 'two-dimensional' fences with equivalent optical porosities. This results in differences in the optimal porosity required to achieve the maximum shear stress reduction coefficient. Results from this study and others in the literature suggest that optimum porosities are approximately 30% and 20% for fences and vegetative windbreaks, respectively, with uniform porosity profiles. For vegetative barriers that are relatively dense near the base or have uniform porosity distributions with height, maximum velocity reductions can be described reasonably well as a function of porosity. Projected plant surface area was also found to be quite useful in describing the maximum velocity reductions obtained in this study when the effect of barrier width was included in the analysis.

Acknowledgments

Appreciation is extended to USDA-ARS, The Robert J. Kleberg, Jr. and Helen C. Kleberg Foundation and the US Agency for International Development, Grant No. DAN-1311-G-SS-1083-00, for supporting this project.

References

Baltaxe, R., 1967. Air flow patterns in the lee of model windbreaks. Arch. Meteorol. Geophys. Bioklimatol. Ser., B 15(3): 287–312.

Bean, A., Alperi, R.W. and Federer, C.A., 1975. A method for categorizing shelterbelt porosity. Agric. Meteorol., 14: 417–429.

Bilbro, J.D. and Fryrear, D.W., 1988. Annual herbaceous windbarriers for protecting crops and soils and managing snowfall. Agric. Ecosys. Environ., 22/23: 149–161.

Borrelli, J., Gregory, J.M. and Abtew, W., 1989. Wind barriers: a re-evaluation of height, spacing and porosity. Trans. ASAE., 32: 2023–2027.

Bradley, E.F. and Mulhearn, P.J., 1983. Development of velocity and shear stress distributions in the wake of a porous shelter fence. J. Wind Eng. Ind. Aerodyn., 15: 145–156.

Caborn, J.M., 1957. Shelterbelts and Microclimate. For. Comm. Bull. No. 29, Edinburgh, 129 pp.

Castro I.P. and Fackrell, J.E., 1978. A note on two-dimensional fence flows, with emphasis on wall constraint. J. Ind. Aerodyn., 3: 1–20.

Counihan, J., Hunt, J.C.R. and Jackson, P.S., 1974. Wakes behind two-dimensional surface obstacles in turbulent boundary layers. J. Fluid Mech., 64: 529–563.

Den Hartog, G., 1973. A field study of the turbulent transport of momentum between the atmosphere and a vegetative canopy. Ph.D. dissertation, University of Guelph, Guelph, Ont.

Fryrear, D.W., 1963. Annual crops as wind barriers. Trans. ASAE, 6: 340–342, 352.

George, E.J., Broberg, D. and Worthington, E.L., 1963. Influence of various types of field windbreaks on reducing wind velocities and depositing snow. J. For., 61: 345–349.

Good, M.C. and Joubert, P.C., 1968. The form drag of two-dimensional bluff plates immersed in turbulent boundary layers. J. Fluid Mech., 31: 547–582.

Hagen, L.J., 1988. Wind erosion prediction system: an overview. ASAE Paper No. 88-2554. St. Joseph, MI: ASAE.

Hagen, L.J. and Skidmore, E.L., 1971. Windbreak drag as influenced by porosity. Trans. ASAE, 14: 464–465.

Hagen, L.J., Skidmore, E.L., Miller, P.L. and Kipp, J.E., 1981. Simulation of effect of wind barriers on airflow. Trans. ASAE, 24: 1002–1008.

Heisler, G.M. and DeWalle, D.R., 1988. Effects of windbreak structure on wind flow. Agric. Ecosys. Environ., 22/23: 41–69.

Jensen, M., 1954. Shelter Effect: Investigations into the Aerodynamics of Shelter and its Effects on Climate and Crops. Danish Technical Press, Copenhagen, 263 pp.

Maki, T. and Allen, L.H.J., 1978. Turbulence characteristics of a single line pine tree windbreak. Proc. Soil Crop Sci. Soc. Fla., 37: 81–92.

Miller, D.R., Rosenberg, N.J. and Bagley, W.T., 1975. Wind reduction by a highly permeable tree shelterbelt. Agric. Meteorol., 14: 321–333.

Nageli, W., 1953. Untersuchungen uber die windverhaltnisse im bereich von schilfrohrwanden (Investigations on the wind conditions in the range of narrow walls of reed.) Mitt. Schweiz. Anst. Forstl. Versuchswesen, 29: 213–266.

Ogawa, Y. and Diosey, P.G., 1980a. Surface roughness and thermal stratification effects on the flow behind a two-dimensional fence. I. Field study. Atmos. Environ., 14: 1301–1308.

Ogawa, Y. and Diosey, P.G., 1980b. Surface roughness and thermal stratification effects on the flow behind a two-dimensional fence. II. A wind tunnel study and similarity considerations. Atmos. Environ., 14: 1309–1320.

Perera, M.D.A.E., 1981. Shelter behind two-dimensional solid and porous fences. J. Wind Eng. Ind. Aerodyn., 8: 93–104.

Plate, E.J., 1971. Aerodynamic Characteristics of Atmospheric Boundary Layers. U.S. Atomic Energy Commission, Critical Review Series. National Technical Information Service, Springfield, VA, 190 pp.

Raine, J.K. and Stevenson, D.C., 1977. Wind protection by model fences in a simulated atmospheric boundary layer. J. Ind. Aerodyn., 2: 159–180.

Schwab, G.O., Frevert, R.K., Edminster, T.W. and Barnes K.K., 1981. Soil and Water Conservation Engineering. Wiley, New York, 525 pp.

Seginer, I., 1975. Atmospheric-stability effect on windbreak shelter and drag. Boundary-Layer Meteorol., 8: 383–400.

Seginer, I. and Sagi, R., 1972. Drag on a windbreak in two-dimensional flow. Agric. Meteorol., 9: 323–333.

Sturrock, J.W., 1969. Aerodynamic studies of shelterbelts in New Zealand—1: Low to medium height shelterbelts in Mid-Canterbury. N. Z. J. Sci., 12: 754–776.

Sturrock, J.W., 1972. Aerodynamic studies of shelterbelts in New Zealand—2: Medium-height to tall shelterbelts in Mid-Canterbury. N. Z. J. Sci., 15: 113–140.

Thom, A.S., 1971. Momentum absorption by vegetation. Q. J. R. Meteorol. Soc., 97: 414–428.

Van Eimern, J., Karschon, R., Razumova, L.A. and Robertson, G.W., 1964. Windbreaks and Shelterbelts. WMO Tech. Note No. 59, 188 pp.

Wilson, J.D., 1985. Numerical studies of flow through a windbreak. J. Wind Eng. Ind. Aerodyn., 21: 119–154.

Wilson, J.D., 1987. On the choice of a windbreak porosity profile. Boundary-Layer Meteorol., 38: 37–49.

Woodruff, N.P., Fryrear, D.W. and Lyles, L., 1963. Engineering similitude and momentum transfer principles applied to shelterbelt studies. Trans. ASAE, 6: 41–47.